SENSITIVITY ANALYSIS OF INTERNAL MAT ENVIRONMENT DURING HOT-PRESSING

*Balázs G. Zombori**

Post-doctoral Research Scientist

Frederick A. Kamke†

Professor and Director
Sustainable Engineered Materials Institute
Virginia Polytechnic Institute and State University
Blacksburg, VA 24061-0503

and

Layne T. Watson

Professor
Departments of Computer Science and Mathematics
Virginia Polytechnic Institute and State University
Blacksburg, VA 24061-0023

(Received July 2002)

ABSTRACT

The effect of several hot-pressing parameters on the internal mat environment was investigated by using a hot-pressing simulation model. The results were compared to experimental data from laboratory-produced flakeboard. The pressing parameters included initial mat moisture content, final panel density, press platen temperature, and press closing time. The variation of temperature and total gas pressure during the press cycle at six points in the vertical mid-plane of a single layer, random mat structure was predicted with the heat and mass transfer model using the different pressing conditions. Twenty-four boards were manufactured according to the same specifications, and the temperature and internal gas pressure were measured with thermocouples and gas pressure probes at the same six locations. The model consistently predicted the major trends during the hot-pressing operation.

The hot-pressing simulation model used in this study was developed based on fundamental engineering principles. The material physical and transport properties were the best available values from the literature or best estimates based on engineering judgment. A sensitivity study assessed the relative importance of the different transport properties during the hot-pressing process. The sensitivity analysis of the model parameters revealed that the thermal conductivity and gas permeability of the mat have the greatest influence on model results. The assessment of these transport properties experimentally, as a function of mat structure, is highly desirable and can considerably improve future model predictions.

Keywords: Wood composite, hot-pressing, modeling, flakeboard, simulation.

INTRODUCTION

A combined stochastic deterministic model has been developed to characterize the random mat formation and internal environment during the hot-pressing of wood-based composites (Zombori et al. 2001, 2002; Zombori 2001). The present paper examines the capability of the model to describe the internal mat environment with specific reference to flakeboard, and compares the simulation results to experimental data. Process simulation models allow operators to gain insight into the effect of certain production

* Dr. Zombori was unfortunately killed in an accident in December 2002.

† Member of SWST.

Wood and Fiber Science, 36(2), 2004, pp. 195–209

parameters on the internal conditions of the mat without extensive experimentation with the production line. Therefore, more informed decisions may be made about the manufacturing parameters to improve panel properties and reduce pressing time. Four production parameters—initial mat moisture content, target panel density, platen temperature, and the press closing time—were investigated for this report. A sensitivity analysis, intended to reveal the relative importance of the model parameters, was also performed.

Many published reports have demonstrated the influence of processing parameters on the physical, mechanical, and dimensional properties of wood-based composites. Most of the cited papers concentrated on four important production parameters: the initial mat moisture content, the target panel density, the platen temperature, and the press closing time. It was recognized by Kelley (1977), in an extensive literature review, the isolation of the effect of individual processing variables on the panel properties is extremely difficult because of the extensive interaction among them.

Maku et al. (1959) reported that the higher the initial mat moisture content, the longer the time needed to vaporize the moisture in the center, resulting in a prolonged temperature plateau. The moisture distribution data provide ample evidence that moisture moves from the surfaces to the middle of the board at the beginning of the hot-pressing process, and from the middle towards the edges at later stages of the press cycle. Strickler (1959) showed that the initial moisture content, and the distribution of the moisture, can affect certain properties of the board (modulus of rupture, modulus of elasticity, internal bond strength, vertical density profile). The authors confirmed that increasing moisture content of the face layer of the board accelerated the temperature rise in the core. It was demonstrated that the maximum initial temperature at the core (temperature achieved at the end of the initial temperature rise) decreases as the average initial moisture content increases. With a very low initial moisture content, no temperature plateau was observed during the experiments.

Kamke and Casey (1988a, b) investigated the effect of initial moisture content, platen temperature, and press closing time on the internal mat conditions during hot-pressing. Thermocouples and gas pressure probes were positioned in the face and core layers of the mat. A higher initial moisture content resulted in faster rate of heat transfer. The temperature in the core of the mats produced with a 15% initial moisture content decreased significantly when venting commenced, indicating that a saturated steam environment was present.

Conflicting results have been reported on the influence of panel density on the maximum initial core temperature. Maku et al. (1959) found a positive relationship between maximum initial core temperature and panel density in the range of 500 to 800 kg/m^3. However, Strickler (1959) did not find any relationship. Both agreed that it took longer to reach the maximum initial core temperature as the panel density increased. Smith (1982) demonstrated that the rate of core temperature rise increased with increasing board density, which is contradictory to the previous experimental findings (Maku et al. 1959; Strickler 1959). The highest density panels (737 kg/m^3) delaminated, even though the resin was completely cured. The low lateral permeability of the panel, with the high density, did not allow the steam to escape, and the high gas pressure overcame the internal bond strength upon press opening.

Maku et al. (1959) found that with increasing platen temperature, from 115°C to 180°C, the core layer loses moisture quickly and the press cycle could be shortened. Kamke and Casey (1988a, b) found that higher platen temperature accelerates the temperature rise in both the face and core locations of the board, and the maximum initial temperatures were also increased. The total pressure responded to the faster temperature rise, as anticipated. The gas pressure increased sooner, and reached a higher peak value with increasing platen temperature.

Smith (1982) found that shorter press closing time resulted in lower core density, consequently increasing the permeability of the mat in the center and allowing the steam pressure to leave the

environment. This result implies that the internal pressure should be lower in the case of a fast press closing time. Data presented by Wang and Winistorfer (2000a) were inconclusive on the influence of press closing time on the internal gas pressure of the mat.

Several other variables can have an influence on the internal environment and board properties. Many researchers reported the possible adjustment of flake dimension and alignment (Bhagwat 1971; Brumbaugh 1960; Dai et al. 2000; Geimer et al. 1975, 1999; Heebink and Hann 1959; Hoglund et al. 1976; Sharma and Sharon 1993; Wang and Lam 1999), and press closing strategies (Smith 1982; Wang and Winistorfer 2000b; Winistorfer and DiCarlo 1988) to control the final properties of the panel. These additional parameters are included in the simulation model. However, comparison with experimental values is not presented here.

MATERIALS AND METHODS

Panel manufacture

The objective of the laboratory-board production was to imitate different industrial pressing situations. Therefore, three initial mat moisture contents (5, 8.5, 12%), three final panel densities (609, 641, 673 kg/m^3 or 38, 40, 42 lb/ft^3), two hot platen temperatures (150, 200 °C), and three press closing times (40, 60, 80 s) were considered in the experimental design. The pressing time was 660 s for boards pressed at 150°C and 540 s for boards pressed at 200°C platen temperature. The pressing time included the different press closing times and a 60-s venting period at the end of the press cycle. The initial press opening was set to 152 mm (6 in.).

The mats were produced from face-layer flakes, which were a mixture of pine and low-density hardwoods, taken from an industrial oriented strandboard facility. The average density of the strands was 466 kg/m^3, and the initial moisture content was 7%. In order to produce mats with 5% initial moisture content, the strands were dried completely, and an adequate amount of water was added to the furnish during the adhesive mixing. Liquid phenol-formaldehyde resin was used with a 4% resins solids loading level. Mats, 610 × 610 mm (24 in. × 24 in.), were hand-formed in a forming box without orientation. The mat was placed in the press on an insulation board in order to avoid the premature heating of the lower regions of the mat, until the thermocouples and pressure probes were placed at the six measuring locations. Then the insulation board was removed, and the mat was compressed to a 19-mm target thickness (0.75 in.) in a computer-controlled hot press. Three panels were produced at each of the pressing conditions. The internal temperature and gas pressure data presented here are the average of the three replicate runs. The finished panels were trimmed at the four edges, then weighed for out-of-press density calculations. Three moisture samples were cut from the center of each board, and the out-of-press moisture content was determined with the oven-dry method.

Temperature and total pressure measurement

Recoverable temperature and pressure probes were built in the laboratory, similar to those commonly used in the wood-based composite industry. The internal gas pressure was determined by piezoelectric pressure transducers (Omega Model: PX 105). The transducers measured total gauge pressure between 0–0.69 MPa (0–100 psi), with an accuracy of ± 2% of full scale. The pressure transducers were connected to the measurement points at the vertical midplane of the mat by stainless steel tubes with a 3.2-mm outside diameter. The stainless steel tubes and the body of the transducers were filled with silicone oil, to reduce response time and protect the diaphragm of the transducers from the hot steam. The temperature was monitored by thermocouples (Omega Model: type-K30AWG). The thermocouple wires were placed inside the stainless steel tubes, which made them completely recoverable.

The probes were positioned horizontally at 76, 152, and 305 mm (3 in., 6 in., 12 in.) from the right edge of the mat and vertically 50 and 20% from the top surface of the mat (Fig. 1). The vertical positioning was accomplished by measur-

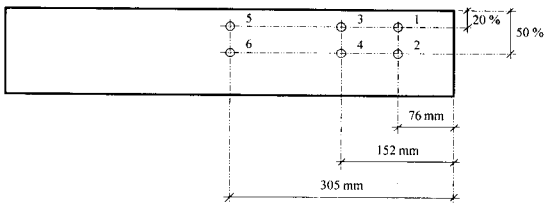

FIG. 1. An elevation view of the mat showing the intended locations of the six thermocouples and pressure probes in the vertical mid-plane. The vertical position is referenced as a percent of the overall thickness at any time during the press cycle.

ing the weight of the deposited strands during the mat formation. Three metal rods were placed within the mat after half the flakes were deposited in the forming box. After forming 80% of the mat by weight, another set of rods was placed to designate the position of the other three probes. This provided internal temperature and gas pressure readings at six points in the vertical mid-plane of the board. Temperature and total pressure data, together with ram pressure and platen position readings, were collected simultaneously at every second during the course of the hot-pressing.

Hot-pressing simulation runs

Hot-pressing of mats, using the same conditions as during the experiments, was simulated with the model (Zombori 2001; Zombori et al. 2002). Mat structures from flakes with face layers dimensional characteristics were constructed with the mat formation model (Zombori et al. 2001). Although special care was taken during the experiments to control the final densities of the panel, the averages of the dry board densities were lower than the intended panel densities. Therefore, the simulated panel densities were adjusted to 600, 633, and 663 kg/m^3 instead of the specified 609, 641, and 673 kg/m^3. The values of the surface and edge boundary transport properties were the base values listed in Table 1. The number of flakes, their cumulative thickness, and cumulative weight were calculated at grid points of a 19 × 19 numerical mesh. The numerical mesh is redefined in two dimensions (mat width and height) for the hot-pressing model.

The heat and mass transfer model provided temperature and total pressure predictions on a 19 × 19 mesh at the vertical mid-plane of the board. The locations of the six measurement probes did not coincide with the mesh points. In order to have comparable data, the predicted results at the mesh points were interpolated to approximate the points corresponding to the probe locations using two-dimensional B-splines. This method allowed direct comparison between the model predictions and experimental measurements.

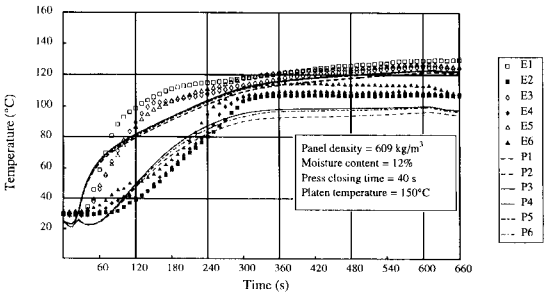

FIG. 2. Plot of temperature at the six measuring locations as a function of press time at 150°C platen temperature. The experimental (E) and model predicted (P) data are overlaid.

RESULTS AND DISCUSSION

Comparison of predicted and measured internal environment

Internal temperature and gas pressure data collected by the hot-pressing experiments at the six probe locations are compared with results predicted by the model. A naming convention was established. Data at probe positions 1, 3, and 5 will be called the face locations, probe positions 2, 4, and 6 will be called the middle locations, and at probe position 6 the core location (Fig. 1). Only the 150°C and 200°C platen temperature conditions are compared in detail because these two data sets provided the most pronounced differences.

Figures 2 and 3 show the temperature and total gas pressure as a function of pressing time

TABLE 1. *The base and perturbed value of the model parameters for the sensitivity study.*

Parameter	Symbol	Base Value	Perturbed Value	Unit
Wood cell-wall conductivity	k_{cw}	0.217	0.3255	J/m/s/K
Permeability of the mat	K_g	1.74×10^{-12}	2.60×10^{-12}	m^2
Diffusion attenuation factor	α	0.5	0.75	
Bound water diffusivity	D_b	3.0×10^{-13}	4.5×10^{-13}	kg s/m^3
Surface heat trans. coef.	H^{face}	75	112.5	J/m^2/s/K
Surface bulk flow coef.	K^{face}	4×10^{-3}	6×10^{-3}	m
Surface diffusion coef.	D^{face}	1.5×10^{-5}	2.25×10^{-5}	m/s
Surface relative humidity	RH^{face}	35	52.5	%
Edge heat trans. coef.	H^{edge}	10	15	J/m^2/s/K
Edge bulk flow coef.	K^{edge}	1×10^{-6}	1.5×10^{-6}	m
Edge diffusion coef.	D^{edge}	1.5	2.25	m/s
Edge relative humidity	RH^{edge}	35	52.5	%
Platen temperature		200	–	°C
Initial mat moisture content		12	–	%
Press closing time		40	–	s
Target panel density		609	–	kg/m^3

for the 150°C platen temperature, while Figs. 4 and 5 depict the same data for the 200°C platen temperature. In general, the model predicted the temperature and pressure trends well, although quantitative differences existed. The temperatures at the three face and three middle locations show very similar behavior. A substantial gradient is formed only in the vertical direction. The pressure behaves in the opposite way, with a gradient built up only from the center of the mat towards the edges in the horizontal direction. The pressure difference between the vertical locations is negligible.

A discrepancy can be observed in the inception of the initial rise of the temperature, especially in the case of the probes located closer to the hot platens (probe positions 1, 3, 5). Plausible explanations are the larger specified press daylight than the uncompressed mat thickness in the press schedule, and the use of caul plates during the tests. The top hot platen contacted the top caul plate approximately 15 s after the start of the schedule, delaying the conduction heat transfer during the experiments. The daylight opening in the model has to be specified as the uncompressed mat thickness for accurate void fraction calculations, which results in an early increase of the temperature. The heating of the caul plate also requires some time in the experiments, while the caul plate is not represented in the model.

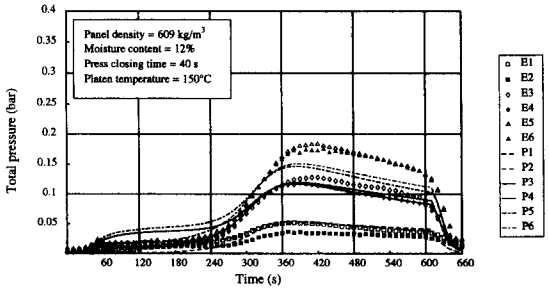

FIG. 3. Plot of total gas pressure at the six measuring locations as a function of press time at 150°C platen temperature. The experimental (E) and model predicted (P) data are overlaid.

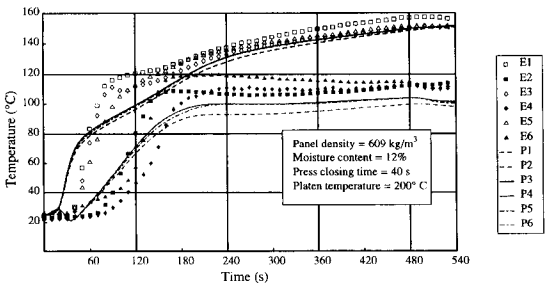

FIG. 4. Plot of temperature at the six measuring locations as a function of press time at 200°C platen temperature. The experimental (E) and model predicted (P) data are overlaid.

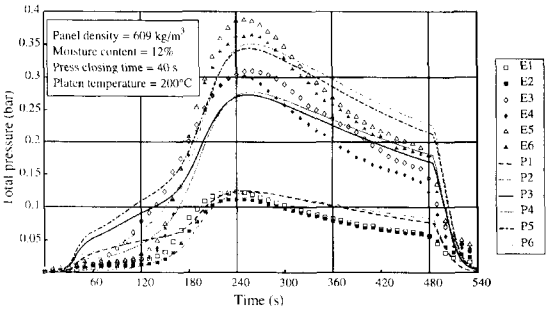

FIG. 5. Plot of absolute total gas pressure at the six measuring locations as a function of press time at 200°C platen temperature. The experimental (E) and model predicted (P) data are overlaid.

The tendency of steeper initial rise with higher platen temperature is well predicted with the model, although the maximum initial temperature is lower at every probe location (Figs. 2 and 4). The predicted middle layer temperatures all tended to level off around 100°C. The higher middle layer temperatures during the experiments can be explained partly by the increased boiling point of water due to the pressurized environment within the mat. The mat core reaches a maximum of 1.2 and 1.4 bar (absolute) total gas pressure during the experiments as depicted in Figs. 3 and 5. The boiling point of water is 105 and 112°C at the respective gas pressures, somewhat lower than the measured plateau temperatures.

The predicted internal pressure starts to build up faster, but the maximum pressure is lower in both cases (Figs. 3 and 5). However, the positions of the peak gas pressures are well predicted. The declining gas pressure in the second part of the press schedule is also present in the model predictions. The total gas pressure is sensitive to the mat permeability (K_g) and the external bulk flow coefficient (K'). The mat permeability can change several orders of magnitude with mat density, primarily due to the size and distribution of the voids between the flakes. Therefore, the vertical density profile has a large influence on both the vertical and horizontal permeability of the mat. The precise prediction of the vertical density profile is an essential condition for accurate pressure, and temperature predictions. The ability of the model to accurately predict the formation of the vertical density profile in the mat will be addressed in a future communication.

The model is able to predict major trends among widely varying pressing conditions. Given the uncertainty of the physical and transport properties of the mat in the literature, the model was considered to perform exceptionally well.

Effect of hot-pressing parameters on the internal environment

The behavior of the core of the mat has a particular significance, since this is the part of the panel with the lowest temperature and least potential for adhesive cure. The data presented are the average of three temperature and internal gas pressure measurements at the core location of the mat (probe position 6) for all the pressing conditions. Figure 6 summarizes the measured and predicted temperature at the core of the board, while Fig. 7 depicts the corresponding total gas pressures. Figure 8 shows the change of the average moisture content of the board during a simulation press run, and also presents the results of the out-of-press moisture content measurements. The error bars depict one standard deviation of the nine out-of-press moisture content measurements.

The most important factor affecting the heat and mass transfer process is the initial moisture content of the mat. The thermal conductivity of the board increases, together with the rate of conduction heat transfer, as the moisture content increases. Increasing moisture content also raises the pressure gradient, which results in an accelerated rate of convection heat transfer by vapor flow. The net result is that the core temperature reaches the boiling point of water at the prevailing internal pressure. Then, after the majority of the water is vaporized, the temperature gradually begins to rise. Obviously, the higher the initial moisture content, the longer will be the temperature plateau. This is clearly the case shown in Fig. 6a, when one compares the measured and predicted core temperatures at 5, 8.5, and 12% initial mat moisture contents. The mag-

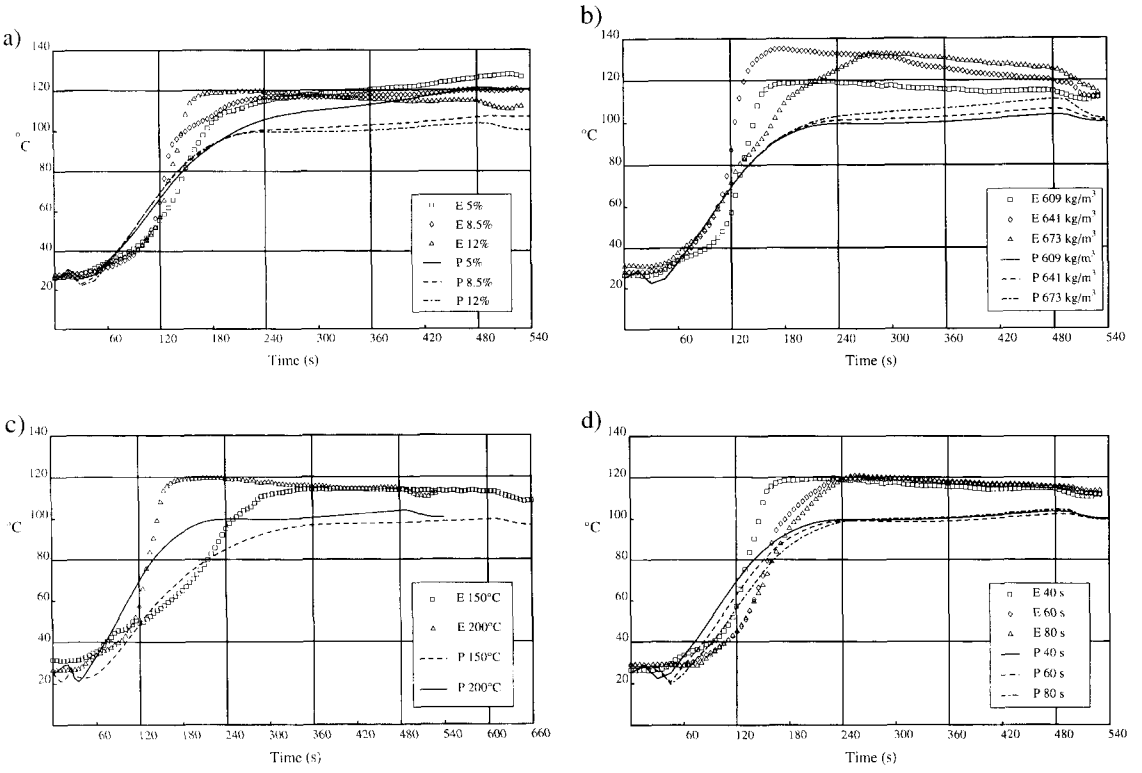

FIG. 6. The effect of mat characteristics and press schedule on the temperature at the core of the mat (probe location 6). The evolution of core temperature with time is depicted as the function of initial mat moisture content (a), board final density (b), press temperature (c), and press closing time (d).The experimentally measured (E) and model predicted (P) data are overlaid. The base conditions are 200°C, 609 kg/m^3, 12%, and 40 s.

nitude of the plateau temperature is controlled by the resistance to gas flow out of the mat. As long as the horizontal permeability is high enough for unrestricted vapor movement at atmospheric pressure, the core temperature plateau will be around 100°C. However, as the permeability decreases, higher internal pressure builds up in the mat. Thus, with sufficient moisture, the saturation temperature at the core rises above 100°C. This behavior was demonstrated during the experiments as well as in the simulations. Increasing the initial mat moisture content increases the amount of water available for vaporization. Consequently, the total pressure increases with increasing moisture content, as was clearly the case demonstrated by the experimental results in Fig. 7a. The model predictions followed this general trend.

The importance of mat permeability is illustrated in Figs. 6 and 7. The measured results for core temperature show a decrease after peak temperature is reached for several of the test cases. This occurs due to the pressure, temperature, and phase equilibrium relationship of a water-vapor dominated system. After the supply of steam from the face region diminishes, and gas pressure drops in the core, the evaporation of bound and liquid water from the core consumes latent heat, thus causing a temperature decrease. If the local mat permeability is low enough, or the mat is narrow (such is the case with a laboratory mat) water vapor pressure drops (Fig. 7), and the temperature drop is rather significant (Fig. 6b). In a low moisture content mat, such as 5%, the core temperature does not decline (Fig. 6a). In this case, the latent heat effect is small.

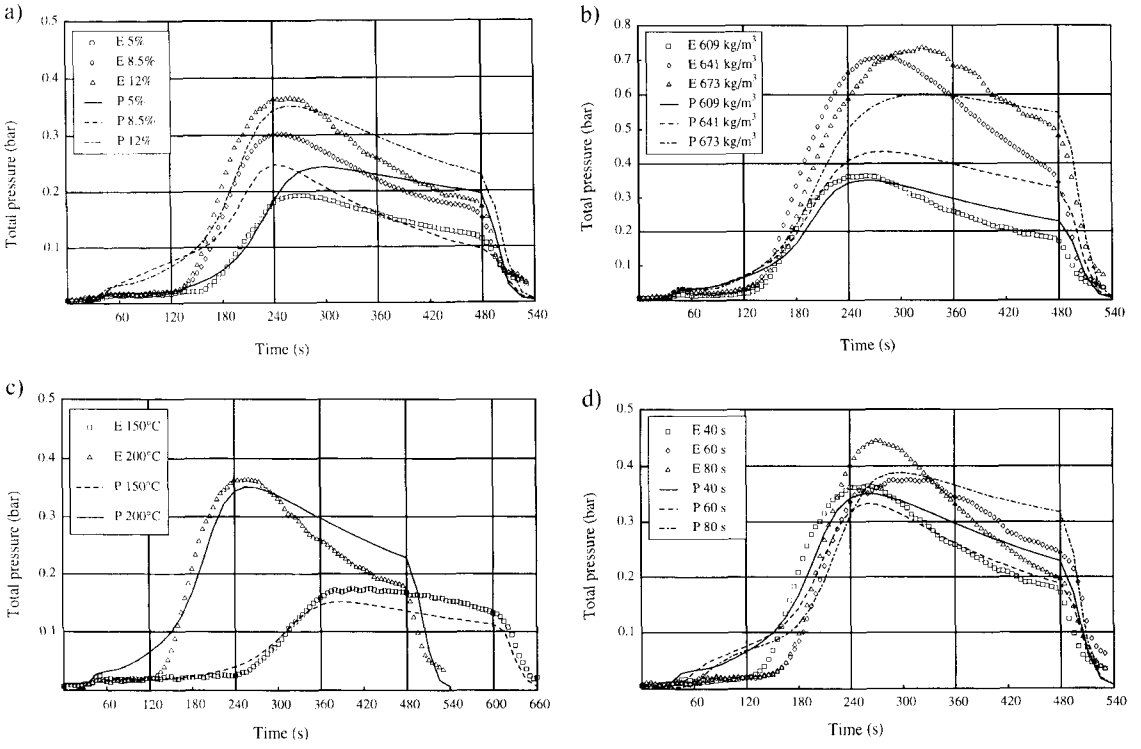

FIG. 7. The effect of mat characteristics and press schedule on the gauge total gas pressure at the core of the mat. The evolution of total gas pressure with time is depicted as the function of mat initial moisture content (a), board final density (b), press temperature (c), and press closing time (d). The experimentally measured (E) and model predicted (P) data are overlaid. The base conditions are 200°C, 609 kg/m^3, 12%, and 40 s.

Figure 8 shows that after the beginning of the press cycle, the mat moisture is slowly depleted. During the press closing time, the permeability of the mat is large and the vapor can easily flow. This is manifested in a fast decrease of moisture in the mat during the press closing time. The moisture depletion slows down after the mat is compressed to the final thickness due to a decline of permeability, As the peak pressure is reached at the core, the moisture depletion is accelerated again. This is most apparent by comparing the occurrence of the pressure peaks in Fig. 7c and the consequent increase of the slope of the moisture content graphs in Fig. 8c at two different platen temperatures. The out-of-press moisture content of the mat obviously depends on the initial mat moisture content. The model could adequately predict the higher out-of-press moisture content with increasing initial mat moisture content as shown in Fig. 8a.

The final density of the board affects the heat transfer process in two opposing ways. First, the thermal conductivity of the mat increases with density, thus accelerating the rate of the conductive heat transfer. Secondly, the increasing density reduces the flow of water vapor through the porous structure of the board, consequently reducing the rate of bulk flow and the associated convective heat transfer. The relative proportions of these two mechanisms will determine the change of the core temperature with final panel density. Additionally, the core temperature is a function of the ratio of the horizontal to the vertical vapor flow. Core temperature tends to be lower as the proportion of horizontal to the vertical flow increases. Escaping vapor effectively cools the core of the mat. Generally, the core

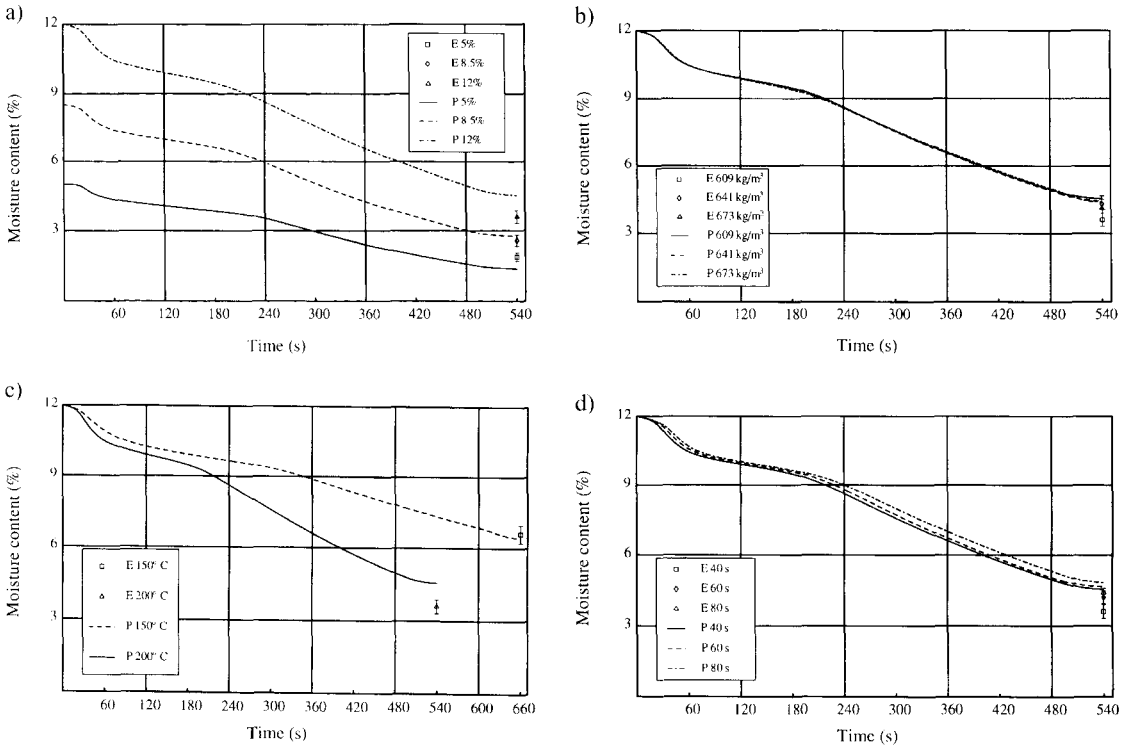

FIG. 8. The effect of mat characteristics and press schedule on the average moisture content of the mat. The evolution of moisture content with time is depicted as the function of initial mat moisture content (a), board final density (b), press temperature (c), and press closing time (d). The base conditions are 200°C, 609 kg/m^3, 12%, and 40 s.

temperature of low-density panels experiences a rapid rise, then levels off quickly close to the boiling point of water. The high-density panels had a slower initial rise, but continued to increase more steadily during the press cycle (Fig. 6b). The model predictions were consistent with these observations, although the effects are not so pronounced. The bulk flow of the gas phase in the horizontal direction is reduced with increasing density due to the reduced amount of free pathways available in the structure. Therefore, the peak of the predicted total pressure in the core of the mat increased together with the density as depicted in Fig. 7b. The core pressure measured at 641 kg/m^3 panel density seemed unjustifiably high. However, the vertical density profile undoubtedly plays an important role in gas pressure development. The shape of the average moisture content plot is not affected by the final panel density (Fig. 8b). The model results and the out-of-press moisture content data show good agreement.

Since the rate of conduction is proportional to the temperature gradient, the higher the platen temperature, the faster the heat transfer process. At 200°C platen temperature, the slope of the core temperature was steeper, and the plateau temperature was reached 120 s earlier than at 150°C (Fig. 6c). The model results predicted the trends in both cases, although the plateau temperatures were lower. The core pressure of panels compressed at higher platen temperature started to rise earlier and faster, and reached a higher maximum than panels pressed at the lower platen temperature (Fig. 7c). This is a clear indication of the interrelationship of the heat and mass transfer phenomena. Figure 8c compares the average moisture content predic-

tions with the out-of-press moisture content data. The predictions are within one standard deviation of the measured out-of-press moisture content at 150°C platen temperature.

The influence of the press closing time may be explained through the changing magnitude of void and contact between the flakes. The more intimate the contact between the flakes, the higher the conductivity. Conversely, the more voids between the flakes, the higher the permeability of the mat. Therefore, fast press closing time will result in close contact at the early stage of the press schedule, increasing the conduction component, but decreasing the convection component. Additionally, the distance between the hot platens reduced faster with decreasing press closing time. The shorter the distance the heat has to be transferred, the faster the core temperature starts to increase. The plateau temperature was not affected by the press closing time (Fig. 6d). This trend was predicted well with the model. The experimental total pressures showed inconsistent behavior in case of the 80-s press closing time (Fig. 7d). The commencement of the pressure rise happens earlier, and the peak is higher than would be expected. While moisture variation or improperly positioned pressure probes within the mat could cause this result, the formation of the vertical density profile can also influence gas flow and pressure in a complex manner. The press closing time seems to have a minute effect on the average moisture content of the mat as shown in Fig. 8d. Faster press closing time resulted in a slightly lower average moisture content than a slower press closing time. The experimental out-of-press moisture data supported these findings.

Sensitivity study

The model has numerous parameters that are based on currently available data in the literature (Zombori 2001; Zombori et al. 2002). These parameters control the magnitude of the transport mechanisms in the model. The aim of the sensitivity study was to gain insight into the relative importance of the model parameters and the contribution of the transport mechanisms during the hot-pressing of wood-based composites.

The relevant hot-pressing parameters were divided into two groups. The first group of parameters represents the transport properties of the mat, such as thermal conductivity (k_{cw}), gas permeability (K_g), diffusivity attenuation factor (α), and bound water diffusivity (D_b). The cell-wall thermal conductivity was chosen to represent the conductivity of the mat, as this parameter has the most direct influence on the mat thermal conductivity. Normally the model calculated the local gas permeability as a function of mat density. In the sensitivity analysis, the gas permeability is kept constant. The transport properties of the mat will determine the speed of the temperature and moisture fronts towards the middle vertically, and towards the edges horizontally, and as such will determine the time dependence of the events within the mat.

The second group of parameters includes the boundary transport properties, such as the external heat transfer coefficient (H^j), external bulk flow coefficient (K^j), external diffusion coefficient (D^j), and the ambient relative humidity (RH^j), where j designates the face (top and bottom) or the edge (left and right) boundary of the mat. The boundary transport coefficients have a pronounced effect on the internal mat environment. They can be derived based on theory for typical boundary layer heat and mass transfer problems. However, for more complicated boundaries, which are present in the case of hot-pressing, they are derived empirically based on experimental data. Because of the lack of published data, the magnitude of the model variables were simply estimated. The movement of heat at the surface is faster than the movement of heat at the edge. This is contrary to the mass transfer, where only a small fraction of the vapor leaves vertically towards the hot platens, and the majority of vapor leaves the mat horizontally towards the edges. The values of the external transport coefficients concur with these observations.

The sensitivity of the model was tested by increasing each transport property by 50%, while leaving the remaining parameters unchanged, as is summarized in Table 1. The responses of three selected variables were considered: core temperature, core total pressure, and average mat mois-

ture content. Sensitivity coefficients for temperature, pressure, and moisture content are defined by Eqs. (1), (2), and (3), respectively.

$$X_T = \phi \frac{\partial T}{\partial \phi}, \quad (1)$$

$$X_P = \phi \frac{\partial P}{\partial \phi}, \quad (2)$$

$$X_M = \phi \frac{\partial M}{\partial \phi}, \quad (3)$$

where ϕ is the parameter, T is temperature, P is total gas pressure, and M is moisture content.

By definition, the sensitivity coefficients indicate the sensitivity of the dependent variable with respect to changes in the model parameter. Monitoring each of the sensitivity coefficients as a function of time provided information about how a change in the transport property affected the selected dependent variables during the press cycle. The sensitivity coefficients are also useful to compare the relative importance of the parameters, when plotted together. If the parameters had been correlated, the sensitivity coefficients would have been proportional to each other. The sensitivity coefficients of the selected variables, as a function of mat transport properties, are shown in Fig. 9. Figures 10 and 11 depict the sensitivity coefficients of the variables as a function of boundary transport properties at the face and edge boundary, respectively.

It is apparent from Fig. 9 that the change of the thermal conductivity of the cell wall (k_{cw}) had the most pronounced effect on all of the dependent variables. The thermal conductivity determines the rate of heat transport by conduction. Therefore, heat from the hot platens reaches the middle of the mat faster, and the initial rise of the core temperature is steeper with increasing cell-wall thermal conductivity (Fig. 9a). This directly affects the total pressure, because latent heat energy is available for water vapor generation, which is subsequently driven to the core of the mat. This results in a larger peak in total pressure in the core of the mat (Fig. 9b). The vapor transport is also accelerated, and the water content of the mat is depleted faster (Fig. 9c). Because of the immense dependence of all of the predicted model variables, the appropriate determination of the cell-wall conductivity has a key importance. The cell-wall thermal conductivity value 0.217 (J/m/s/K) is the most widely used (Siau 1995).

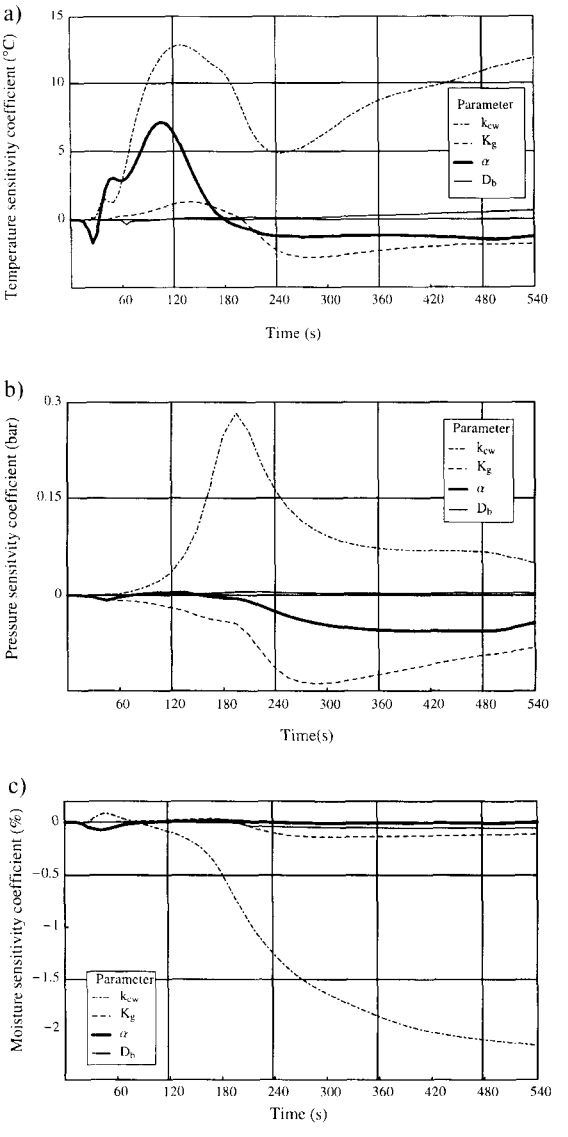

FIG. 9. The sensitivity coefficients of core temperature (a), total gas pressure (b), and average moisture content with time, as a function of the transport properties of the mat, at probe location 6.

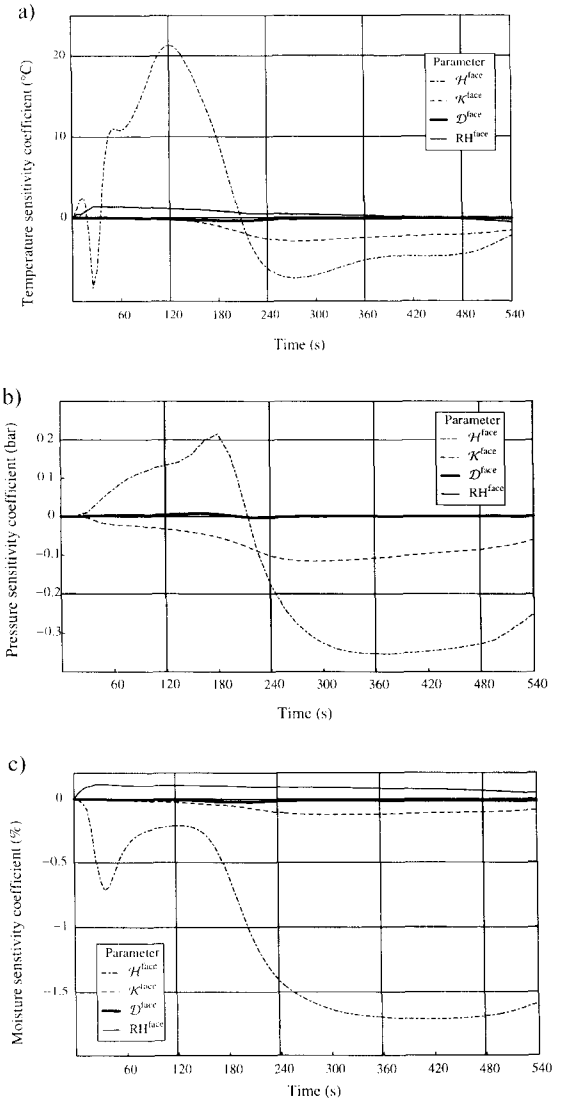

FIG. 10. The sensitivity coefficients of core temperature (a), total gas pressure (b), and average moisture content with time, as a function of the transport properties of the mat, at the top and bottom faces of the mat.

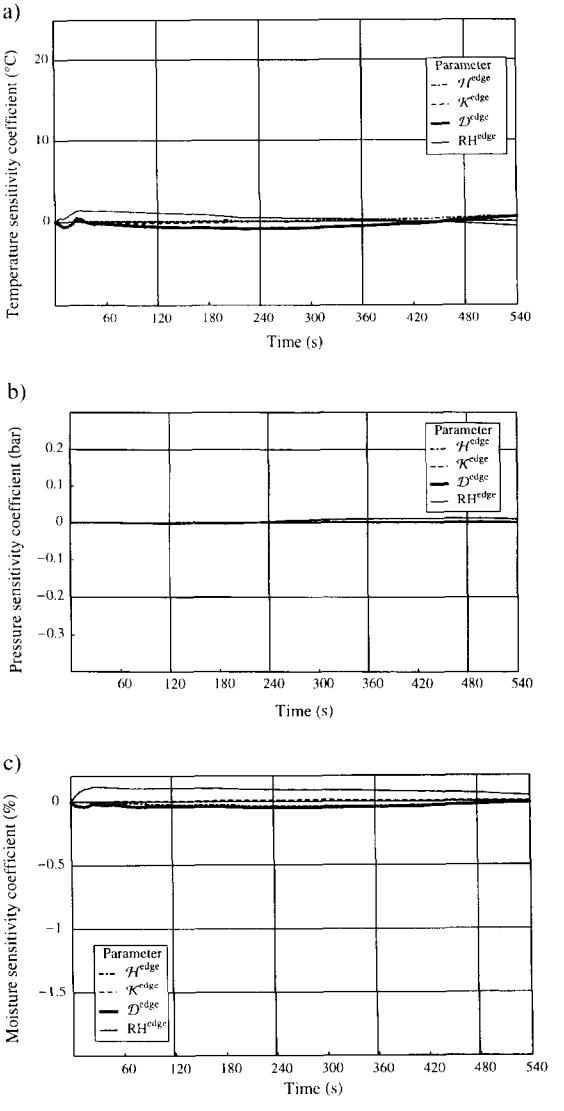

FIG. 11. The sensitivity coefficients of core temperature (a), total gas pressure (b), and average moisture content with time, as a function of the transport properties of the mat, at the left and right edges of the mat.

However, the influence of the transient structure on the thermal conductivity of the mat requires further experimental work.

The selected model variables are all sensitive to the gas permeability (K_g) of the mat. The gas permeability determines the ease of bulk flow within the mat structure. The expected effect is that, as the permeability of the mat and consequent rate of the gas flow are increased, the total pressure becomes smaller in the core of the mat (Fig. 9b). The permeability of the mat must be highly variable, with a strong relation to flake dimensions, flake orientation, mat density, and perhaps other mat structure variables. There is limited literature available on the structure dependence of the mat permeability. The uncer-

tainty of the mat permeability is large, and therefore, a comprehensive experiment would be highly desirable.

The diffusivity attenuation factor (α) determines the openness of the porous structure for gas phase diffusion, and can have a value between 0 and 1. Generally, the attenuation factor has a smaller effect on the core pressure and average moisture content than the gas permeability (Figs. 9b and 9c). This implies that the bulk flow has the primary role in the mass transport within the mat structure. Notice that the influence of α on core temperature is considerable at the beginning of the hot-pressing process (Fig. 9a).

The bound water diffusivity determines the rate of diffusion of bound water in the cell-wall matrix. The bound water diffusion is slow compared to the bulk flow and gas phase diffusion mass transfer. None of the variables are sensitive to the small perturbation of the bound water diffusivity (D_b). Therefore, the precise determination of the temperature and moisture dependence of the bound water diffusivity will not significantly improve the model predictions. A constant value of 3×10^{-13} (kg s/m^3), as reported by Schajer et al. (1984), was used in the model.

The external heat and mass transfer coefficients, together with the relative humidity of the ambient air, determine the rate of the heat and moisture transfer between the surroundings and the boundaries of the mat. Figures 10 and 11 summarize the sensitivity coefficients of the core temperature, core total pressure, and average moisture content for a 50% increase of the external heat and mass transfer coefficients at the face and at the edge of the mat. A comparison of Figs. 10 and 11 confirms the intuition that the surface external transfer properties have a more pronounced effect on the variables at the core of the mat than the edge external transfer properties. The dimension of the board is smaller in the vertical than in the horizontal direction. Therefore, the temperature and pressure at the core of the board are more sensitive to the surface external transfer coefficients than to the edge external transfer coefficients.

The external heat transfer coefficient at the face of the board controls the rate of heat transported from the hot platens to the surface of the board (H^{face}). This boundary property has the most pronounced influence on the dependent variables (Fig. 10). Heat from the hot platens can reach the surface of the board and can propagate to the center faster as H^{face} increases. This will result in an earlier, and more intense, vapor generation in the mat (Fig. 10b). The edge external heat transfer coefficient H^{edge} has no significant influence on the variables at the core of the board. The heat transfer from the hot platens to the surface of the board is fast, while heat transfer at the edge of the mat is far slower. Given this consideration, and the measured temperatures in the experimental mats, the external heat transfer coefficient in the model was estimated to be 75 J/m^2/s/K and 10 J/m^2/s/K at the surface and at the edge of the board, respectively.

Vapor leaves the mat either by bulk flow, due to total pressure differential, or diffusion, due to partial pressure differential, between the outermost point of the mat and the environment. The magnitude of the bulk flow at the surface and at the edge of the mat is controlled by the external bulk flow coefficients (K^{face}, K^{edge}), and the diffusion by the external diffusion coefficients (D^{face}, D^{edge}).

The edge external bulk flow coefficient is several orders of magnitude larger than that for the surface and has a constant value, representing the rapid steady escape of vapor horizontally, while the surface external bulk flow coefficient is a function of the type of boundary at the hot platens. The surface value is very low when solid metal plates form the boundary, presumably allowing only a small amount of vapor to escape. If a wire mesh were placed between the hot platens and the surface of the mat, the surface external bulk flow coefficient would be much larger. During the experiments, solid metal plates were used at the surface boundary, and therefore, the value of the external bulk flow coefficient at the surface was selected to be seven orders of magnitude smaller (3.3×10^{-13} m) than at the edge ($1 \times {}^{-6}$ m). The previously established general observation that the surface external coefficient is more influential on the model variables also applies here, but the reasons are

different (see Figs. 10 and 11). The very high edge external bulk flow coefficient forms no hindrance for the free escape of vapor at the edge. This situation does not change considerably with the increase of the coefficient. Therefore, none of the variables was influenced noticeably by the change of this parameter. However, the surface bulk flow coefficient was set to a low value in the model, inducing a high resistance to vapor flow. Small changes of this resistance can have a large effect on the variables, especially on the total gas pressure as depicted in Fig. 10b. In this case, the vapor is released not only at the edges, but also towards the metal plates. The vapor will follow this new shorter pathway to escape to the environment, creating a smaller vapor pressure in the core of the mat. This vertically escaping vapor takes its energy content to the surroundings, thus reducing the core temperature (Fig. 10a). A considerable amount of moisture leaves the mat towards the metal platens, which is apparent by the decrease of the moisture sensitivity coefficient as the surface external bulk flow coefficient is increased (Fig. 10c).

The magnitude of the diffusion at the boundaries of the board is controlled by the external coefficients (D^{face}, D^{edge}). The external diffusion coefficient at the surface of the mat is estimated to be far lower (0.5×10^{-6} m/s) than at the edge boundary (1.5 m/s). The contribution of diffusion is negligible compared to the contribution of bulk flow in the external diffusion coefficients.

The magnitude of the partial pressure gradients is a function of the relative humidity at the boundaries (RH^{face}, RH^{edge}). The total pressure of the surroundings remains constant at the atmospheric pressure (101,325 Pa) during the hot-pressing process. The relative humidity will determine the vapor content of the ambient air and consequently the partial vapor and air pressure components of the total atmospheric pressure. In other words, the vapor partial pressure gradient is decreased and the escape of vapor to the environment is retarded. The air partial pressure differential is increased and the depletion of air content of the mat is accelerated by diffusion. The relative humidity has no effect on the total pressure; consequently, it has no effect on the bulk flow. The variables are not sensitive to the relative humidity of the environment (Figs. 10 and 11). This observation supports the assertion that the main mode of mass transport between the mat and the environment is bulk flow, and the role of diffusion is secondary. The relative humidity was set to 35% at the boundaries in the model. This relative humidity value was measured in the laboratory environment surrounding the hot press.

The sensitivity analysis indicates that the thermal conductivity and gas permeability are the two mat transport properties that have the greatest effect on the model predictions. Additionally, the external heat transfer and bulk flow coefficients at the surface can alter the core temperature and pressure predictions considerably. The experimental determination of these properties is beyond the scope of the present paper, but in the authors' opinion, it should be the subject of further study.

SUMMARY AND CONCLUSIONS

Heat and mass transfer mechanisms, which are induced by the hot-pressing process, have been integrated into a general model, whose derivation was described previously. Several simplifying assumptions were made to facilitate the numerical solution of the heat and mass transfer equations. An extensive set of experimental data of internal mat conditions during hot-pressing was presented. These results represent a broad range of conditions that are typically encountered in the manufacture of oriented strandboard. The trends predicted by the model were in agreement with all of the experimental data presented here. Quantitative differences between the predicted and measured results are attributed to incomplete information regarding several transport properties. The sensitivity analysis of the model parameters indicated that the experimental determination of the thermal conductivity and the gas permeability as a function of mat structure is highly desirable, and will improve the model predictions.

ACKNOWLEDGMENTS

The financial support by the USDA National Research Initiative Competitive Grant Program,

Grant No. 97-35504-4697. USDA CSREES, Special Grant No. 2002-34489-12079, and the Wood-Based Composite Center, Blacksburg, Virginia are greatly appreciated. Special thanks to Harrison Sizemore and Bob Carner for helping to install the measurement system.

REFERENCES

BHAGWAT, S. 1971. Physical and mechanical variations in cottonwood and hickory flakeboards made from flakes of three sizes. Forest Prod. J. 21(9):101–103.

BRUMBAUGH, J. 1960. Effect of flake dimension on properties of particleboard. Forest Prod. J. (5):243–246.

DAI, C., B. KNUDSON, AND R. WELLWOOD. 2000. Research and development in oriented strandboard (OSB) processing. Proc. 5th Pacific Rim Bio-Based Composites, December 10–13, 2000, Canberra, Australia, Pp. 556–563.

GEIMER, R. L., H. M. MONTREY, AND W. F. LEHMAN. 1975. Effects of layer characteristics on properties of three-layer particleboard. Forest Prod. J. 25(3):19–29.

———, J. W. EVANS, AND D. SETIABUDI. 1999. Flake furnish characterization: Modeling board properties with geometric descriptors. USDA For. Serv. Res. Paper FPL-RP-577. USDA For. Prod. Lab., Madison, WI.

HEEBINK, B. G., AND R. A. HANN. 1959. How wax and particle shape affect the stability strength of oak particle boards. Forest Prod. J. 9(7):197–203.

HOGLUND, H., U. SHOLIN, AND G. TISTAD. 1976. Physical properties of wood in relation to chip refining. Tappi 59(6):144–147.

KAMKE, F. A., AND L. J. CASEY. 1988a. Gas pressure and temperature in the mat during flakeboard manufacture. Forest Prod. J. 38(3):41–43.

———, AND ———. 1988b. Fundamentals of flakeboard manufacture: internal mat conditions. Forest Prod. J. 38(6):38–44.

KELLEY, M. W. 1977. Critical literature review of relationships between processing parameters and physical properties of particleboard. USDA. Forest Serv., For. Prod. Lab., Gen. Tech. Rep. FPL-10.

MAKU, T., R. HAMADA, AND H. SASAKI. 1959. Studies on the particleboard. Report 4: Temperature and moisture distribution in particleboard during hot-pressing. Wood Research, Kyoto University Report 434–46.

SCHAJER, G. S., M. A. STANISH, AND F. KAYIHAN. 1984. A computationally efficient approach to drying of hygroscopic and non-hygroscopic porous materials. Proc. ASME Annual Meeting, 84-WA/HT-13, New Orleans, LA.

SHARMA, V., AND A. SHARON. 1993. Optimal orientation of flakes in oriented strandboard (OSB). Exp. Mech. 32(2): 91–98.

SIAU, J. F. 1995. Wood: Influence of moisture on physical properties. Department of Wood Science and Forest Products, Virginia Polytechnic Institute and State University, Blacksburg, VA.

SMITH, D. C. 1982. Waferboard press closing strategies. Forest Prod. J. 32(3):40–45.

STRICKLER, M. D. 1959. Effects of press cycle and moisture content on properties of Douglas-fir flakeboard. Forest Prod. J. 9(7):203–215.

WANG, K., AND F. LAM. 1999. Quadriatic RSM models of processing parameters for three-layer oriented flakeboards. Wood Fiber Sci. 31(2):173–186.

WANG, S., AND P. M. WINISTORFER. 2000a. Consolidation of flakeboard mats under theoretical laboratory pressing and simulated industrial pressing. Wood Fiber Sci. 32(4): 527–538.

———, AND ———. 2000b. Fundamentals of vertical density profile formation in wood composites. Part II. Methodology of vertical density formation under dynamic conditions. Wood Fiber Sci. 32(2):220–238.

WINISTORFER, P. M., AND D. DICARLO. 1988. Furnish moisture content, resin nonvolatile content, and assembly time effects on properties of mixed hardwood strandboard. Forest Prod. J. 38(11/12):57–62.

ZOMBORI, B. G. 2001. Modeling the transient effects during the hot-pressing of wood-based composites. Ph.D. Dissertation, Virginia Polytechnic Institute and State University, Blacksburg, VA.

———, F. A. KAMKE, AND L. T. WATSON. 2001. Simulation of the mat formation process. Wood Fiber Sci. 33(4): 564–580.

———, ———, AND ———. 2002. Simulation of the internal mat conditions during the hot-pressing process. Wood Fiber Sci. 35(1):2–23.